DALTON
FULL PAPER

Chromium-(II) and -(III) over a planar oxo surface modelled by calix[4]arene anions: redox chemistry and formation of Cr–C functionalities

Joëlle Hesschenbrouck,[a] Euro Solari,[a] Carlo Floriani,*[a] Nazzareno Re,[b] Corrado Rizzoli[c] and Angiola Chiesi-Villa[c]

[a] *Institut de Chimie Minérale et Analytique, BCH, Université de Lausanne, CH-1015 Lausanne, Switzerland. E-mail: carlo.floriani@icma.unil.ch*
[b] *Facoltà di Farmacia, Università degli Studi "G. D'Annunzio", I-66100 Chieti, Italy*
[c] *Dipartimento di Chimica, Università di Parma, I-43100 Parma, Italy*

Received 25th October 1999, Accepted 24th November 1999

The metallation of [*p*-Bu^{t}calix[4](ONa)$_2$(OMe)$_2$] **1** was performed using [$CrCl_3(THF)_3$] and the resulting complex [Cr{*p*-Bu^{t}calix[4](O)$_2$(OMe)$_2$}(Cl)(THF)] **2** allowed entry into low valent and organometallic chemistry of chromium. In the presence of strong bases or nucleophiles the ligand underwent demethylation exemplified by the reaction of **2** with pyridine, which led to [C_5H_4NMe][Cr{*p*-Bu^{t}calix[4](O)$_3$(OMe)}Cr(py)(Cl)] **3**. The alkylation of **2** was successful only when the concurrent reduction to Cr^{II} was irrelevant, in which case the two well characterized organometallic derivatives [Cr{*p*-Bu^{t}calix[4](O)$_2$(OMe)$_2$}(Mes)] **4** [Mes = 2,4,6-$Me_3C_6H_2$] and [Cr{*p*-Bu^{t}calix[4](O)$_2$-(OMe)$_2$}(η^5-C_5H_5)] **5** were obtained. None of them showed, even under photochemical or thermal forced conditions, any sign of reactivity, due to the kinetic inertness of the d^3 configuration. Complex **2** was easily reduced to the chromium(II) derivative [Cr{*p*-Bu^{t}calix[4](O)$_2$(OMe)$_2$}(THF)] **6**, which underwent facile oxidative functionalization. The reaction with O_2 led to an unprecedented di-μ-oxo chromium(IV) derivative, [Cr_2{*p*-Bu^{t}calix[4](O)$_2$(OMe)$_2$}$_2$-(μ-O_2)] **7**, which displays a ferromagnetic coupling between the two d^2 centres. The proposed structures are supported by X-ray analyses of complexes **2**–**4**, **6** and **7**.

Introduction

Calix[4]arene derived anions comprise a set of oxygen donor atoms preorganized in a quasi-planar fashion particularly appropriate for studying the redox and organometallic chemistry of early transition metals.[1–3] The partial alkylation of the O_4 set allows one to tune the charge of the O_n macrocycle and, by consequence, the degree of functionalization of the metal.[3] A nearly planar preorganized O_4 set binding chromium should be considered as a molecular model of a variety of chromium–oxide extended structures.[4] It is well known that chromium and chromium oxides supported on other oxides, such as Al_2O_3, are important catalysts for a wide variety of reactions.[5,6] This report is focused on the synthesis of Cr^{III}– and Cr^{II}–calix[4]-arene derivatives, which can be considered appropriate starting materials for developing chromium chemistry over the oxo-surface modelled by the calix[4]arene skeleton in its cone conformation. The Cr–calix[4]arene chemistry is limited so far to a single report on octahedral Cr^{III} encapsulated by two fused calix[4]arene moieties,[7] while there is a lack of appropriate starting compounds for entering the chromium redox and organometallic chemistry supported by the calix[4]arene macrocycle. The reactivity of the Cr–calix[4]arene derivatives has been exemplified, studying a few redox and organometallic reactions. The supporting ligand, adapted for Cr^{III} and Cr^{II}, is the alkylated form of calix[4]arene displayed in Chart 1.

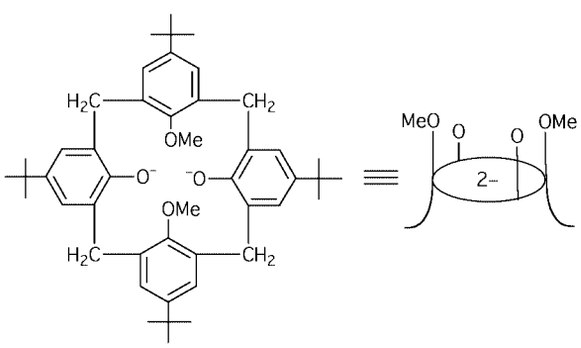

Chart 1

Experimental

General

All reactions were carried out under an atmosphere of purified nitrogen. Solvents were dried and distilled before use by standard methods. The ^{1}H NMR and IR spectra were recorded on AC-200, DPX-400 Bruker, and Perkin-Elmer FT 1600 instruments, respectively. Magnetic susceptibility measurements were made using an MPMS5 SQUID susceptometer (Quantum Design Inc.) operating at a magnetic field strength of 1 kOe. Corrections were applied for diamagnetism calculated from Pascal constants.[8] Effective magnetic moments were calculated from $\mu_{eff} = 2.828(\chi_{Cr}T)^{1/2}$, where χ_{Cr} is the magnetic susceptibility per chromium. Fitting of the magnetic data by the theoretical expression was performed by minimizing the agreement factor, defined as $\Sigma[(\chi_i^{obs}T_i - \chi_i^{calc}T_i)^2/(\chi_i^{obs}T_i)^2]$, through a Levenberg–Marquardt routine. The syntheses of *p*-Bu^{t}calix[4]-(OMe)$_2$(OH)$_2$[9] and its disodium salt **1**[3] were performed according to the literature.

Syntheses

Compound 2. The compound [$CrCl_3(THF)_3$] (5.53 g, 14.8 mmol) was added to a white suspension of **1**·THF (11.71 g,

14.8 mmol) in THF (200 cm^3). The mixture was stirred overnight and THF was evaporated. Then *n*-hexane (150 cm^3) was added, and a green product was collected and extracted with diethyl ether (250 cm^3). The green solid was collected and dried *in vacuo* (11.38 g, 92%). Crystals suitable for X-ray analysis were grown in a THF–ether solution (Found C, 71.08; H, 8.22. **2**, $C_{50}H_{66}ClCrO_5$ requires C, 71.96; H, 7.97%). IR (Nujol, $\tilde{\nu}_{max}$/cm^{-1}): 1594w, 1361m, 1333s, 1294m, 1261m, 1206s, 1161m, 1117s, 1090m, 1006s, 922w, 867m, 839s, 798w, 784w and 552w.

Compound 3. A green solution of compound **2** (2.49 g, 3.0 mmol) in pyridine (70 cm^3) was refluxed overnight. A black microcrystalline product was collected, washed with pentane (50 cm^3) and dried *in vacuo* (1.46 g, 52%). Crystals suitable for X-ray analysis were grown in a pyridine solution (Found C, 72.24; H, 7.29; N, 3.99. **3**, $C_{56}H_{68}ClCrN_2O_4$ requires C, 73.06; H, 7.44; N, 3.04%). IR (Nujol, ν_{max}/cm^{-1}): 1630w, 1602m, 1580w, 1359s, 1322s, 1282s, 1256m, 1206s, 1167w, 1120w, 1098m, 1069w, 1042w, 1017s, 989w, 912w, 872m and 844m.

Compound 4. Mesityllithium (0.54 g, 4.29 mmol) was added to a toluene (150 cm^3) solution of compound **2** (3.58 g, 4.29 mmol). The mixture was stirred overnight and LiCl removed by filtration. Toluene was evaporated *in vacuo* and pentane (100 cm^3) added. The green product was collected and dried *in vacuo* (1.98 g, 55%). Crystals suitable for X-ray analysis were grown in a toluene–hexane solution (Found C, 78.28; H, 8.53. **4**, $C_{55}H_{69}CrO_4$ requires C, 78.07; H, 8.22%). IR (Nujol, $\tilde{\nu}_{max}$/cm^{-1}): 1589w, 1361m, 1311s, 1272m, 1206s, 1161m, 1117m, 1091m, 1044w, 1000s, 922w, 872m, 839m, 800m, 767w, 711w and 539m.

Compound 5. The compound NaCp·DME (0.96 g, 5.4 mmol) was added to a green solution of **2** (4.50 g, 5.3 mmol) in THF (150 cm^3). The mixture was stirred overnight and NaCl removed by filtration. A brown solution was obtained; THF was evaporated *in vacuo* and pentane (100 cm^3) added. The orange product was collected and dried *in vacuo* (1.72 g, 40%) (Found C, 78.16; H, 8.46. **5**, $C_{51}H_{63}CrO_4$ requires C, 77.34; H, 8.02%). IR (Nujol, $\tilde{\nu}_{max}$/cm^{-1}): 1600w, 1378w, 1360m, 1309s, 1272m, 1211m, 1156w, 1124w, 1083w, 1016m, 993m, 917w, 870m, 843m, 813m, 779w and 534w.

Compound 6. Sodium (0.52 g, 22.5 mmol) and naphthalene (1.30 g, 10.1 mmol) were added to a green solution of compound **2** (18.75 g, 22.5 mmol) in THF (300 cm^3). The mixture was stirred overnight and NaCl removed by filtration. The brown solution was concentrated, *n*-hexane (100 cm^3) added and a blue product collected and dried *in vacuo* (10.50 g, 58%). Crystals suitable for X-ray analysis were grown in a THF–*n*-hexane solution (Found C, 75.19; H, 8.75. **6**, $C_{50}H_{66}CrO_5$ requires C, 75.16; H, 8.32%). IR (Nujol, $\tilde{\nu}_{max}$/cm^{-1}): 1594w, 1389w, 1356m, 1319s, 1300s, 1200m, 1161w, 1117w, 1089w, 1067s, 1037m, 1006s, 894m, 867m, 822w, 800m and 539m.

Compound 7. A solution of compound **6** (1.90 g, 2.4 mmol) was refluxed in toluene (100 cm^3) for 2 h, then toluene was distilled and *n*-hexane (100 cm^3) added. The blue green solution was stirred under O_2 (27 cm^3, 1.2 mmol). A black crystalline product was collected and dried *in vacuo* (0.507 g, 25%) (Found C, 75.22; H, 8.58. **7**, $C_{52}H_{72}CrO_5$ requires C, 75.33; H, 8.75%). IR (Nujol, $\tilde{\nu}_{max}$/cm^{-1}): 1587w, 1392w, 1361m, 1284s, 1250s, 1208s, 1121m, 1002m, 977m, 907w, 874w, 807m, 803m, 768w, 756m, 736m, 708m, 641w, 577w, 535s, 482w and 449m.

X-Ray crystallography

Suitable crystals were mounted in glass capillaries and sealed under nitrogen. Crystal data and details associated with data collection are given in Table 1. Data for complexes **2**, **3**, **7** were collected on a Mar345 imaging plate system. Cell refinements and data reductions were performed with the MARHKL version 1.9.1 suite of programs.[10] Data for **4**, **6** were collected on a KumaCCD diffractometer. Cell measurement, cell refinement and data reduction were performed with KM4RED.[11] The crystal quality was tested by ψ scans showing that crystal absorption effects could be neglected for all complexes. The function minimized during the least-squares refinements was $\Sigma w(\Delta F^2)^2$. Anomalous scattering corrections were included in all structure factor calculations.[12b] Scattering factors for neutral atoms were taken from ref. 12(*a*) for non-hydrogen atoms and from ref. 13 for H. Structure solutions were based on the observed reflections [$I > 2\sigma(I)$] while the refinements were based on the unique reflections having $I > 2\sigma(I)$. The structures were solved by the heavy-atom method starting from a three-dimensional Patterson map.[14] Refinements were done by full matrix least squares first isotropically and then anisotropically for all non-H atoms except for the disordered atom. The hydrogen atoms of all complexes were put in geometrically calculated positions and introduced in the refinements as fixed atom contributions ($U_{iso} = 0.05$ Å^2). For all complexes the final difference maps showed no unusual features, with no significant peaks above the general background. All calculations were performed by using SHELXL93[15] implemented on a QUANSAN personal computer equipped with an INTEL PENTIUM II processor.

CCDC reference number 186/1744.

See http://www.rsc.org/suppdata/dt/a9/a908499a/ for crystallographic files in .cif format.

Results and discussion

The transmetallation of compound **1** is quite straightforward using [$CrCl_3(THF)_3$]. The reaction led to six-co-ordinate Cr^{III} in complex **2**, having a quite distorted octahedral co-ordination. The reactivity of **2** can be moderately affected by the use of strong bases or nucleophiles under drastic conditions. In fact, on refluxing **2** in pyridine the demethylation of one of the methoxy groups and the formation of **3** were obtained (Scheme 1).

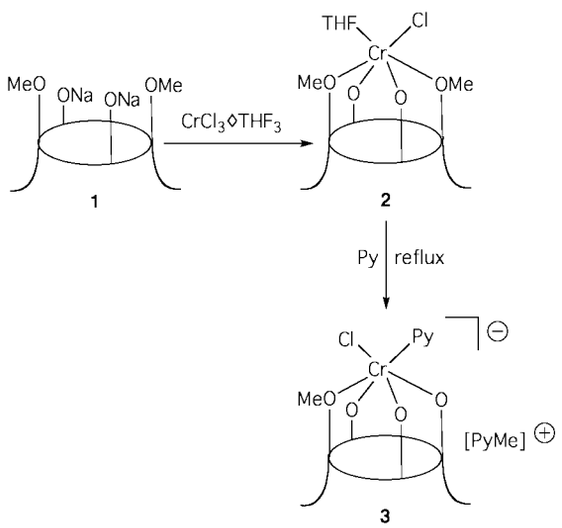

Scheme 1

Dealkylation of [*p*-Bu^{t}calix[4](O)$_2$(OMe)$_2$]$^{2-}$ occurs when high valent metals are used.[2f,3a–c] The structures of **2** and **3** are shown in Figs. 1 and 2, respectively. Selected bond distances and angles are quoted in Table 2. Relevant conformational parameters within the Cr–calix[4]arene units are given in Table 3. The labelling scheme adopted for the calixarene macrocycle is depicted in Chart 2.

Crystals of complex [Cr{*p*-Bu^{t}calix[4](O)$_2$(OMe)$_2$}(Cl)(THF)] (Fig. 1) contain Et_2O in a 1:2 molar ratio. The co-

Table 1 Experimental data for the X-ray diffraction studies on crystalline complexes **2**–**4**, **6** and **7**

	2[a]	**3**[b]	**4**[c]	**6**[d]	**7**[e]
Formula	$C_{50}H_{66}ClCrO_5 \cdot 2C_4H_{10}O$	$C_{56}H_{68}ClCrN_2O_4 \cdot C_5H_5N$	$C_{55}H_{69}CrO_4 \cdot 2C_7H_8$	$C_{50}H_{66}CrO_5 \cdot 2C_4H_8O$	$C_{92}H_{116}Cr_2O_{10} \cdot 2C_6H_{14}$
Formula weight	982.8	999.7	1030.4	943.3	829.1
Crystal system	Monoclinic	Monoclinic	Triclinic	Orthorhombic	Monoclinic
Space group	13.529(3)	15.408(3)	13.542(2)	12.526(2)	14.605(3)
a/Å	30.221(5)	23.553(5)	15.295(2)	19.174(2)	18.269(4)
b/Å	13.998(4)	16.322(3)	15.682(2)	21.933(2)	17.875(4)
c/Å			81.43(2)		
α/°	103.76(2)	109.26(2)	81.68(2)		93.85(3)
β/°			69.06(2)		
γ/°	5559(2)	5591.8(20)	2985.0(8)	5267.7(11)	4758.6(18)
U/Å^3	173	185	143	143	143
T/K	$P2_1/c$ (no. 14)	$P2_1/n$ (no. 14)	$P\bar{1}$ (no. 2)	$P2_12_12_1$ (no. 18)	$P2_1/c$ (no. 14)
Z	4	4	2	4	2
μ/cm^{-1}	2.95	2.92	2.30	2.59	2.76
Total reflections	48947	42565	22564	38710	24743
Unique total	10134	10930	11844	12824	7423
R(int)	0.063	0.059	0.026	0.042	0.090
Observed reflections [$I > 2\sigma(I)$]	6982	7865	9595	10284	4187
R	0.070	0.067	0.067	0.061	0.066
*wR*2	0.181	0.163	0.166	0.142	0.165

[a] The C(38)–C(40) methyl carbon atoms of the *tert*-butyl group associated to the **C** ring and the C(48) carbon atom of the THF molecule showed high thermal parameters indicating the presence of disorder. The best fit was found by splitting the atoms over two positions (A and B) isotropically refined with site occupation factors of 0.5. One Et_2O solvent molecule was also affected by disorder, which was solved by splitting the O(7), C(55)–C(58) atoms over two positions (A and B) isotropically refined with site occupation factors of 0.5. During the refinement the C–O and C–C bond distances within the disordered solvent molecule were constrained to 1.43(1) and 1.54(1) Å respectively. [b] The methyl carbon atoms of the *tert*-butyl group associated to the **A** and **B** rings showed high thermal parameters indicating the presence of disorder. The best fit was found by splitting the atoms over two positions (A and B) isotropically refined with site occupation factors of 0.7 and 0.3 respectively for C(30)–C(32) and 0.5 for C(34)–C(36). [c] The C(34)–C(36) and C(38)–C(40) methyl carbon atoms of the *tert*-butyl group associated to the **B** and **C** rings were statistically distributed over two positions (A and B) isotropically refined with site occupation factors of 0.6 and 0.4, respectively. The guest toluene molecule was also affected by disorder, which was solved by splitting the C(56)–C(62) atoms over three positions (A, B and C) isotropically refined with site occupation factors of 0.5, 0.25 and 0.25, respectively. During the refinement the aromatic rings of the "partial" toluene molecules were constrained to have D_{6h} symmetry [C–C 1.39(1) Å]. [d] Refinement was carried out straightforwardly. Since the space group is polar, the crystal chirality was tested by inverting all the coordinates (x, y, $z \longrightarrow -x$, $-y$, $-z$) and refining to convergence again. The resulting R values ($R = 0.067$, $wR2 = 0.154$) indicated the original choice should be considered the correct one. [e] The methyl carbon atoms of the *tert*-butyl group associated to the **A** ring showed high thermal parameters indicating the presence of disorder. The best fit was found by splitting the C(30)–C(32) atoms over two positions (A and B) isotropically refined with site occupation factors of 0.5. The *n*-hexane solvent molecule was also affected by severe disorder, which was solved by splitting the C(47), C(48) atoms over three positions (A, B and C) and the C(49)–C(52) atoms over two positions (A and B) isotropically refined with the site occupation factors of 0.5 for the A and B positions of C(30)–C(32), 0.4 and 0.6 for the A and B positions respectively of C(49)–C(52), 0.2, 0.6 and 0.2 for the A, B and C positions respectively of C(47), C(48). During the refinement the C–C bond distances within the disordered solvent molecule were constrained to be 1.54(1) Å.

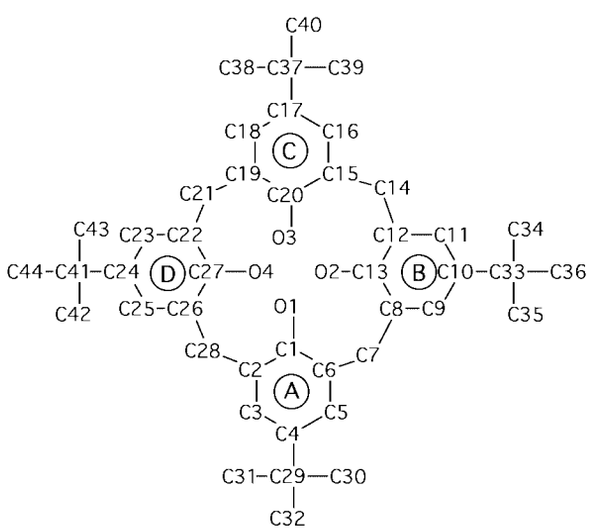

Chart 2

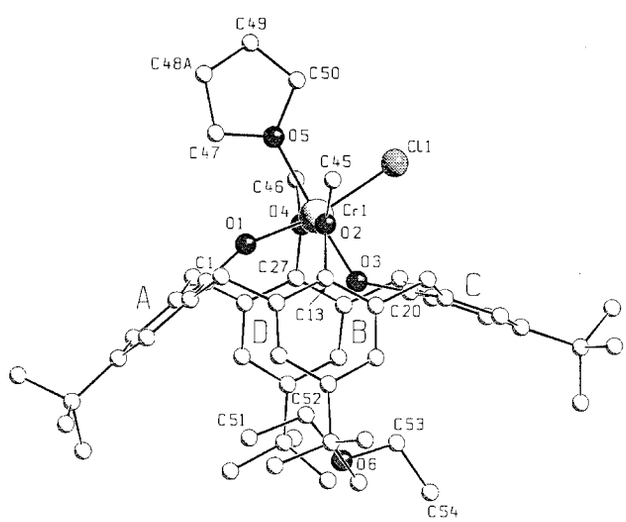

Fig. 1 A SCHAKAL[16] view of complex **2**. Disorder affecting the **C** butyl group and the THF molecule has been omitted for clarity.

ordination polyhedron around chromium is a slightly distorted octahedron, with the best equatorial plane defined by the O(1), O(3), O(5), Cl(1) atoms (the deviations from the planarity range from −0.036(3) to 0.038(3) Å for O(3) and O(1), respectively) and the O(2) and O(4) atoms in the axial positions. The metal is displaced by 0.022(1) Å from the mean equatorial plane toward O(2). The *cis* arrangement of the THF and chloride ligands removes the planarity of the O_4 core, which shows remarkable tetrahedral distortions (Table 3). The very short Cr–O1 and Cr–O3 [Cr–O_{av}, 1.868(3) Å] distances[17] are consistent with a significant metal–oxygen π bonding (Table 2). The

Table 2 Selected bond distances (Å) and angles (°) for complexes **2**–**4**, **6**, **7**

2					
Cr(1)–Cl(1)	2.307(1)	Cr(1)–O(3)	1.866(3)	Cl(1)–Cr(1)–O(5)	85.9(1)
Cr(1)–O(1)	1.870(3)	Cr(1)–O(4)	2.065(3)		
Cr(1)–O(2)	2.072(3)	Cr(1)–O(5)	2.181(3)		
3					
Cr(1)–Cl(1)	2.337(1)	Cr(1)–O(3)	1.866(3)	Cl(1)–Cr(1)–N(1)	89.0(1)
Cr(1)–O(1)	1.886(2)	Cr(1)–O(4)	1.911(2)		
Cr(1)–O(2)	2.239(2)	Cr(1)–N(1)	2.162(3)		
4					
Cr(1)–O(1)	1.890(2)	Cr(1)–O(3)	1.842(2)	Cr(1)–C(47)	2.068(2)
Cr(1)–O(2)	2.084(2)	Cr(1)–O(4)	2.072(2)		
6					
Cr(1)–O(1)	1.960(2)	Cr(1)–O(3)	1.961(2)	Cr(1)–O(5)	2.297(2)
Cr(1)–O(2)	2.089(2)	Cr(1)–O(4)	2.091(2)		
7					
Cr(1)–O(1)	1.853(4)	Cr(1)–O(3)	1.856(4)	Cr(1)–O(5)	1.726(4)
Cr(1)–O(2)	2.462(3)	Cr(1)–O(4)	2.058(3)	Cr(1)–O(5′)	1.888(3)
Cr(1)–O(5)–Cr(1′)	97.4(2)				

A prime denotes the transformation $1 - x, -y, 1 - z$.

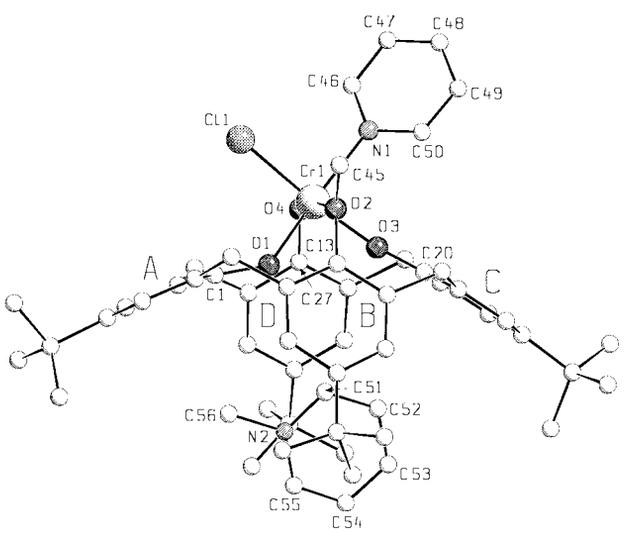

Fig. 2 A SCHAKAL view of complex **3**. Disorder affecting the **A** and **B** butyl groups has been omitted for clarity.

calixarene macrocycle assumes a flattened elliptical conformation with the **C** ring roughly parallel to the mean "reference" plane through the methylene C(7), C(14), C(21), C(28) carbon atoms (Table 3). This conformation allows an Et_2O molecule to be accommodated inside the calixarene cavity. The host–guest interactions should be described in terms of CH–π interactions[18] occurring between the C(51) methyl and the C(52) methylene carbons of the guest and the **A**, **B** and **D** rings. C(51)···C_A, 3.750(7)–3.919(7); C(51)···$\mathbf{A}_{centroid}$, 3.586(7); H(511)···$\mathbf{A}_{centroid}$, 2.64; C(52)···C_B, 3.803(7)–4.213(7); C(52)···$\mathbf{B}_{centroid}$, 3.757(5); H(522)···$\mathbf{B}_{centroid}$, 2.78; C(52)···C_D, 3.858(6)–4.213(5); C(52)···$\mathbf{D}_{centroid}$, 3.746(7); H(521)···$\mathbf{D}_{centroid}$, 2.80 Å.

Complex **3** crystallizes from pyridine which is present in the crystals in 1:1 molar ratio. The structure of the anion is shown in Fig. 2. It is quite similar to that of **2**, where a pyridine molecule replaces the THF molecule in the co-ordination sphere of the metal. The O(1), O(3), Cl(1), N(1) set of donor atoms defines the equatorial plane of a distorted octahedron, while O(2) and O(4) atoms are in the axial positions. The metal protrudes by 0.149(1) Å from the mean equatorial plane toward O(4). The six-co-ordination of the metal removes, as is usual, the planarity of the O_4 core (the deviations from planarity range from −1.304(3) to 0.274(2) Å). The Cr–O bond distances involving O(1), O(3) and O(4) oxygen atoms [mean value 1.893(12) Å] reveal the existence of a significant π bonding, which is absent for the methoxy group [Cr–O(2), 2.239 Å][7,17] (Table 2). The elliptical conformation of the macrocycle is similar to that observed in **2**, the main difference consisting in the narrowing of the dihedral angle between the "reference" plane and the **A** and **B** rings. The methylpyridinium cation guest molecule enters the cavity approximately parallel to the **B** and **D** rings (dihedral angles 30.4(1) and 18.3(1)°, respectively) and perpendicular to the **A** and **C** rings (dihedral angles 76.2(1) and 89.0(1)°, respectively). This arrangement could favour CH_3–π host–guest interactions between the protons of the C(56) methyl group of toluene and the **A** aromatic ring [C(56)···C_A, 3.309(4)–3.761(5); C(56)···$\mathbf{A}_{centroid}$, 3.286(6); H(561)···$\mathbf{A}_{centroid}$, 2.49 Å].

The magnetic behaviour of compounds **2** and **3** does not show any anomaly, being in agreement with the expected high spin state for octahedral d^3 (see below).

Complex **2** is a starting material for access to organometallic functionalization and the lower oxidation state of chromium. The alkylation of **2** was successful only when using LiMes (Mes = mesityl) and NaCp, and led to clean synthesis of the mesityl and the cyclopentadienyl derivatives **4** and **5**, respectively (Scheme 2). In the case of other alkylating agents the concurrent reduction reaction or the intrinsic thermal instability of the Cr^{III}–alkyl functionality prevented the isolation of clean compounds. The stability of **4** and **5** could be associated to the steric protection by the axial mesityl or the cyclopentadienyl ligand. Even under drastic thermal conditions or with inserting substrates, we did not observe any reactivity of **4**, in accordance with its expected kinetic inertness. The structure of **4** is displayed in Fig. 3.

Complex **4** crystallizes with toluene in a 1:2 molar ratio. One toluene molecule is hosted in the calixarene cavity. Chromium exhibits a distorted trigonal bipyramidal co-ordination, with O(1), O(3) and C(47) defining the equatorial plane and O(2), O(4) in the axial positions. The metal is displaced by 0.025(1) Å from the equatorial plane toward O(4). The O_4 core shows remarkable tetrahedral distortions ranging from −0.398(2) to 0.234(2) Å, the normal to the mean O_4 plane being nearly parallel to the Cr–C(47) vector (dihedral angle 7.7(1)°). The Cr–O

Table 3 Comparison of relevant conformational parameters within the Cr(calix[4]arene) units for complexes **2**–**4**, **6** and **7**

	2	**3**	**4**	**6**	**7**
(a) Distances (Å) of atoms from the O_4 mean plane					
O(1)	−0.494(3)	−0.136(2)	−0.204(2)	−0.048(2)	0.422(4)
O(2)	0.488(3)	0.274(2)	0.234(2)	0.047(2)	−0.415(4)
O(3)	−0.484(3)	−1.304(3)	−0.398(2)	−0.048(2)	0.422(4)
O(4)	0.491(3)	0.247(2)	0.223(2)	0.048(2)	−0.492(4)
Cr	0.702(1)	0.442(1)	0.378(1)	0.093(1)	0.865(1)
(b) Dihedral angles (°) between planar moieties[a]					
E ∧ **A**	138.4(1)	157.1(1)	131.1(1)	125.5(1)	120.5(1)
E ∧ **B**	113.5(1)	111.7(1)	112.4(1)	116.0(1)	114.2(1)
E ∧ **C**	162.8(1)	148.4(1)	151.1(1)	124.6(1)	119.7(1)
E ∧ **D**	113.4(1)	116.5(1)	112.6(1)	117.0(1)	173.0(1)
A ∧ **C**	121.2(1)	125.5(1)	102.1(1)	109.8(1)	119.7(2)
B ∧ **D**	133.1(1)	131.8(1)	135.0(1)	127.0(1)	107.2(2)
(c) Contact distances (Å) between *para*-carbon atoms of opposite aromatic rings					
C(4)···C(17)	9.894(6)	10.090(5)	9.637(5)	8.560(6)	7.865(8)
C(10)···C(24)	7.454(6)	7.472(5)	7.276(4)	7.840(6)	9.361(8)

[a] **E** (reference plane) refers to the least-squeares mean plane defined by the C(7), C(14), C(21), C(28) bridging methylenic carbons.

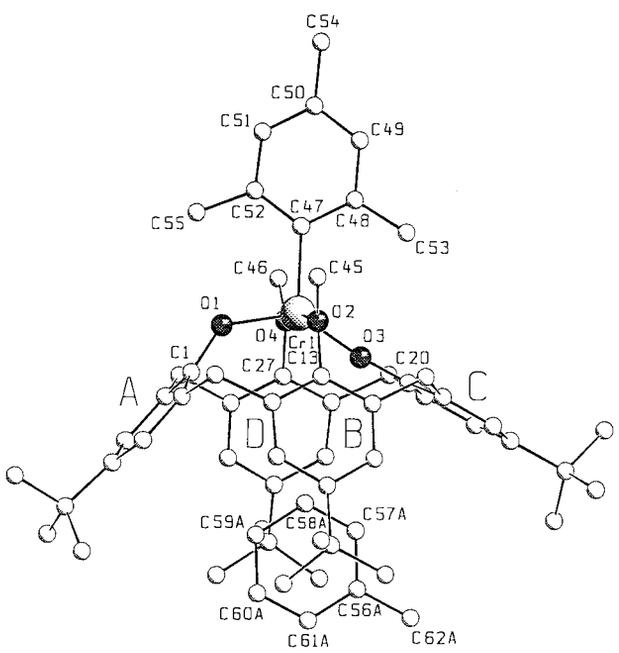

Fig. 3 A SCHAKAL view of complex **4**. Disorder affecting the **B** and **C** butyl groups and the toluene guest molecule has been omitted for clarity.

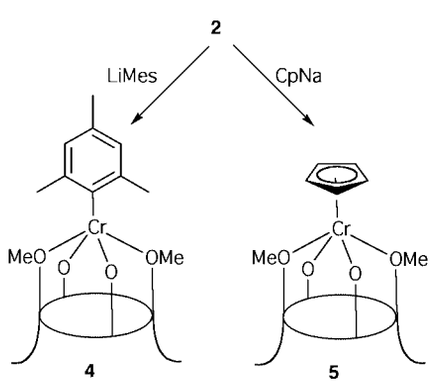

Scheme 2

distances (Table 2) vary from 1.890(2) to 2.084(2) Å, according to the presence, for the former value, of π bonding. The Cr–C bond distance, 2.068(2) Å, is quite normal for Cr–aryl derivatives.[19] The mean plane through the mesitylene aromatic ring is oriented to form a dihedral angle of 21.2(1)° with the Cr, O(1), O(3), C(47) mean plane.†

The metal sitting inside a quite protected cavity is rather inaccessible to any substrate, thus almost completely unreactive. Although the metal is formally five-co-ordinate, the steric hindrance of the mesityl group, along with the C–H–O interactions between the *o*-methyl groups from the mesityl and the oxygens from the calix[4]arene, are probably responsible for the elliptical conformation of the calix[4]arene skeleton. Similar elliptical conformations have been observed in the case of six-co-ordinated metals (Table 3).[3b] As in the latter case, the resulting cavity is suitable for hosting a toluene molecule.

The reactivity of the chromium(III) derivatives so far reported is very low, even under thermal or photochemical forced conditions. In order to increase the reactivity of the metal center in the Cr–calix[4]arene moiety we moved to the by far less kinetically inert Cr^{II}. Compound **2** undergoes one-electron reduction to **6** using sodium in the presence of naphthalene in THF. Complex **6** was isolated as blue crystals, while all the Cr^{III}–calix[4]arene derivatives are green. The magnetic measurement is consistent with high-spin d^4 with a normal paramagnetic behaviour (see below). Its structure shows the five-co-ordination of the metal atom, achieved by the presence of a THF molecule (Fig. 4).

Complex **6** crystallizes with THF in a 1 : 2 molar ratio. One of the two THF molecules of crystallization is hosted in the calixarene cavity. The metal exhibits a square pyramidal co-ordination, the oxygen atoms from the O_4 core defining the equatorial plane. The O_4 core shows small but significant tetrahedral distortions (Table 3), the metal being displaced by 0.093(1) Å from the mean plane through it. The Cr–O(5) vector forms a dihedral angle of 8.2(1)° with the normal to the O_4 mean plane. The trend in the Cr–O bond distances (Table 2), appearing in two sets, is the same as discussed for complexes **2**–**4**. The macrocycle shows a nearly regular cone conformation (Table 3) due to the presence of a five-co-ordinate metal.[3b]

† Short intramolecular contacts are observed involving the H(551) and H(531) protons from methyl groups of mesitylene and O(1) and O(3) atoms respectively (C(55)···O(1), 2.922(3); H(551)···O(1), 2.06; C(53)···O(3), 3.190(3); H(531)···O(3), 2.27 Å). Additional contacts involve the H(451) and H(461) protons from the methoxy groups of calixarene, which are oriented to point toward the centroid of the mesitylene ring: C(45)···C_{Mes}, 3.344(4)–5.154(4); C(45)···$Mes_{centroid}$, 4.115(4); H(451)···$Mes_{centroid}$, 3.27; C(46)···C_{Mes}, 3.296(4)–5.053(4); C(46)···$Mes_{centroid}$, 4.021(4); H(461)···$Mes_{centroid}$, 3.18 Å.

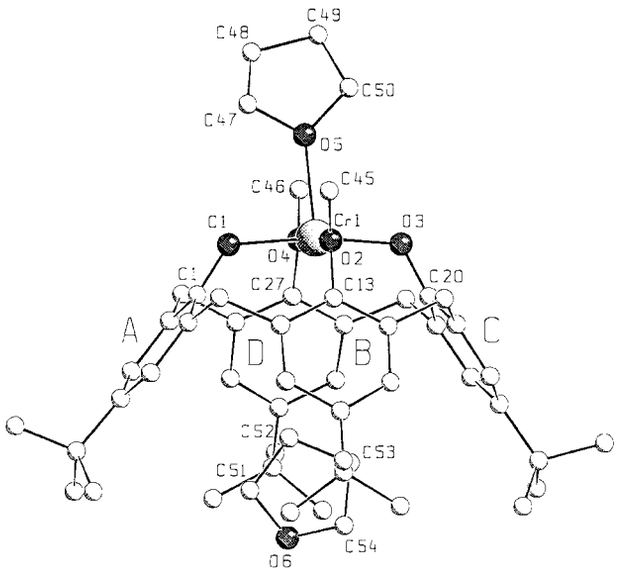

Fig. 4 A SCHAKAL view of complex **6**.

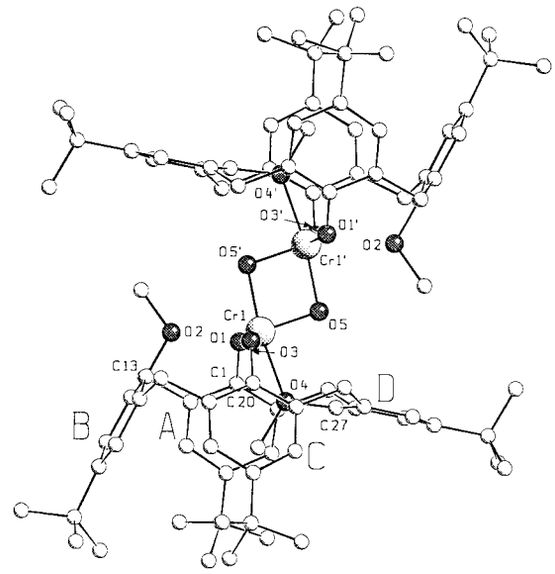

Fig. 5 A SCHAKAL view of complex **7**. Disorder affecting the **A** butyl group has been omitted for clarity. A prime denotes the transformation $1 - x, -y, 1 - z$.

Complex **6** is air sensitive. It absorbs O_2 in the O_2:Cr molar ratio of 1:2, so exemplifying the tendency of Cr to move up in oxidation state. The reaction with O_2 should be carried out on **6** previously refluxed in toluene. This operation probably removes the THF molecule and makes **6** more reactive. In addition, THF can be engaged in an oxidative degradation assisted by the chromium complex. According to the plausible pathway drawn in Scheme 3, we suppose the formation of a bridged peroxodi-

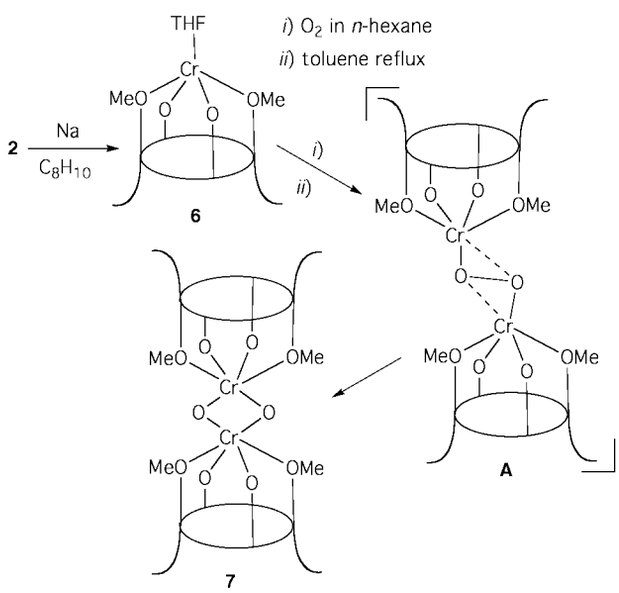

Scheme 3

chromium complex **A**, which undergoes cleavage of the O–O bond, thus forming a quite unique di-μ-oxo-Cr^{IV} derivative, **7**.[20]

The structure of complex **7** consists of centrosymmetric dimers (Fig. 5), where the two metal ions are asymmetrically bridged by the oxo groups, thus forming a Cr_2O_2 ring, which is planar for reasons of symmetry. Chromium exhibits a severely distorted octahedral co-ordination, the best equatorial plane being defined by the O(2), O(4), O(5), O(5′) oxygen atoms [deviations ranging from −0.002(4) to 0.003(4) Å]. The metal lies exactly in the equatorial mean plane. The Cr–O(5) bond distances involving the μ-oxo anion are significantly different [Cr–O(5), 1.726(4); Cr–O(5′), 1.888(3) Å]. The Cr–O bond distances involving the calixarene oxygen atoms fall in a rather wide range (Table 2). This fact may be the consequence of remarkable intraligand steric hindrance mainly involving the C(21), C(28), C(45) carbon atoms and the O(5) oxygen atoms: C(21)···O(5), 3.312(7); H(212)···O(5), 2.71; C(28)···O(5), 3.311(7); H(281)···O(5), 2.72; C(45)···O(5′), 3.011(6); H(451)···O(5′), 2.39 Å (primes indicate the transformation $1 - x, -y, 1 - z$). The very long Cr–O(2) distance would suggest the absence of any bonding between the two atoms, leaving the methyl group free to rotate and be accommodated inside the calix cavity. The intramolecular "host–guest" interactions could be interpreted in terms of CH_3–π interactions[18] occurring between the protons of the C(46) methyl group and the aromatic **A**, **B** and **C** rings: C(46)···C_A, 3.094(8)–4.068(8); C(46)···$\mathbf{A}_{centroid}$, 3.336(8); H(462)···$\mathbf{A}_{centroid}$, 2.81; C(46)···C_B, 3.670(8)–4.428(8); C(46)···$\mathbf{B}_{centroid}$, 3.813(8); H(461)···$\mathbf{B}_{centroid}$, 2.89; C(46)···C_C, 3.074(8)–3.930(8); C(46)···$\mathbf{C}_{centroid}$, 3.278(8); H(463)···$\mathbf{C}_{centroid}$, 2.71 Å. The conformation of the calix skeleton in **7** is remarkably different from those in complexes **2**–**4** and **6**, in particular the **D** ring is nearly parallel to the "reference" plane (Table 3).

The magnetic susceptibilities of complexes **2**–**7** were measured in the temperature range 1.9–300 K. The magnetic moments of **2**–**5** are essentially constant in the whole range of temperature, with a value of *ca.* 3.8 μ_B at room temperature showing only an almost negligible decrease below 2 K (due to a small zero-field splitting), thus indicating a high spin, $S = 3/2$, state for these monomeric chromium(III) compounds. The magnetic moment of **6** has a value of *ca.* 4.2 μ_B at room temperature and is essentially constant throughout the whole range of temperatures with a small decrease below 10 K (due to zero-field splitting), thus indicating a high spin, $S = 2$, state for this monomeric chromium(II) species. The temperature dependence of the magnetic moment of the bis-μ-oxo dimer **7** shows a steady increase from room temperature down to about 20 K and then a slight decrease (Fig. 6). The increase is due to a ferromagnetic coupling between the two chromium(IV) centres, while the decrease at low temperatures is due to zero field splitting, which may be significant for chromium(II) species. The data were fitted using the spin Hamiltonian[21] (1) where

$$\hat{H} = g\beta\boldsymbol{H}(\hat{S}_1 + \hat{S}_2) + D[\hat{S}_{1z'} - \tfrac{2}{3}] + D[\hat{S}_{2z'} - \tfrac{2}{3}] - 2J(\hat{S}_1 \cdot \hat{S}_2) \quad (1)$$

$S_1 = S_2 = 1$ are the spins of the two chromium(IV) ions, D the zero-field-splitting parameter and J the Heisenberg coupling constant between the two centres. The magnetic susceptibility at each temperature point was calculated by use of the

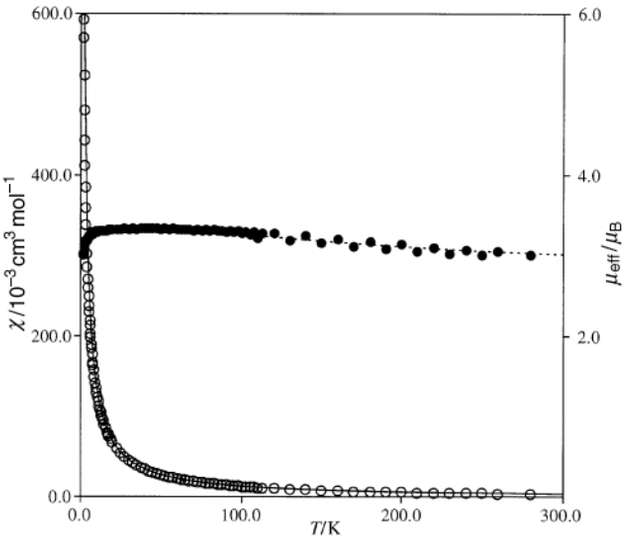

Fig. 6 Magnetic susceptibility (○) and magnetic moment (●) as a function of the temperature for complex **7**.

Van-Vleck equation[21] (2) where N is Avogadro's number, k the

$$\chi = M/H = [N\Sigma_i(-\mathrm{d}E_i/\mathrm{d}H)\exp(-E_i/kT)]/[H\Sigma_i \exp(-E_i/kT)] \quad (2)$$

Boltzmann constant and H the applied field. The energy levels of the tetramers, E_i, are evaluated by diagonalizing the Hamiltonian matrix in the uncoupled spin functions basis set. The calculated best-fit parameters are: $g = 1.92$, $J = +40.4$ cm^{-1} and $D_{Cr} = -5.9$ cm^{-1}. To the best of our knowledge, bis-μ-oxo-chromium(IV) dimers have not been magnetically characterized. However, the ferromagnetic coupling constants have been frequently observed for other μ-oxo bridged vanadium(III) dimers (with the same d^2–d^2 metal configuration)[22] and interpreted in terms of the interaction between the magnetic orbitals.[22,23]

In order to perform extended Hückel calculations,[24] the Cr{*p*-Bu^{t}calix[4](O$_2$)(OMe)$_2$} fragment was slightly simplified by replacing it by two phenoxo and two anisole molecules within a C_{2v} geometry. This simplified model retains the main features of the whole ligand. In particular, the geometrical constraints on the O$_4$ set of donor atoms has been maintained by fixing the geometry of the phenoxo and ether molecules to the experimental X-ray values.

The frontier orbitals of the Cr{*p*-Bu^{t}calix[4](O)$_2$(OMe)$_2$} fragment are reported on the left of Fig. 7 and consist of four low-lying metal-based orbitals. We can distinguish two low-lying almost degenerate orbitals, *i.e.* the 1b$_1$(d_{xz}), pointing in the plane of the two methoxy ligands, and the 1a$_1$(d_{z^2}). Owing to the stronger interaction with the phenoxo ligands in the *yz* plane, the 1b$_2$(d_{yz}) orbital is *ca*. 0.8 eV higher in energy than the 1b$_1$(d_{xz}). The 1a$_2$(d_{xy}) orbital is also raised in energy by the π interactions with the p orbitals of the unmethylated O atoms and lies only 0.2 eV lower than the 1b$_2$.

The presence of a low-lying 1a$_1$(d_{z^2}) orbital in this fragment allows the easy co-ordination by σ ligands, as in the mesityl complex **4**. The Cr{*p*-Bu^{t}calix[4](O)$_2$(OMe)$_2$} fragment may also employ the two d_π orbitals, 1b$_1$(d_{xz}) and 1b$_2$(d_{yz}), in binding a suitable π ligand. This has been exemplified by the co-ordination of the cyclopentadienyl anion in **5**.

The orbital interaction diagram between the [Cr{*p*-Bu^{t}calix-[4](O)$_2$(OMe)$_2$}]$^+$ cation and the Cp$^-$ ligand is shown in Fig. 7. On the extreme right we present the frontier orbitals of Cp$^-$, *i.e.* the a$_2$″, e$_1$″ and e$_2$″ of, respectively, σ, π and δ symmetry with respect to the Cr–Cp axis. The filled e$_1$″ interact with the metal 1b$_1$(d_{xz}) and 1b$_2$(d_{yz}) orbitals respectively, while a weaker interaction is observed between the lower lying a$_2$″ and the metal

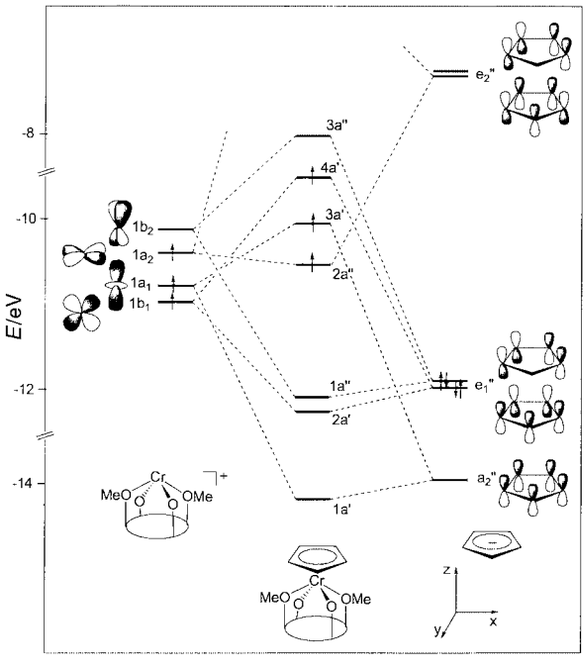

Fig. 7 Orbital interaction diagram for complex **5**.

1a$_1$(d_{z^2}). Finally a weak δ interaction is also observed between the empty e$_2$″ and the metal 1a$_2$(d_{xy}). Although the metal centre would be expected to be reactive toward both electrophiles and nucleophiles, the steric bulkiness of the cyclopentadienyl ligand prevents any reaction in the *exo*-calix position.

Acknowledgements

We thank the Fonds National Suisse de la Recherche Scientifique (Bern, Switzerland, Grant No. 20-53336.98) and Action COST D9 (European Program for Scientific Research, OFES No. C98.008) for financial support.

References

1 C. Floriani, *Chem. Eur. J.*, 1999, **5**, 19 and references therein.
2 (*a*) L. Giannini, E. Solari, S. Dovesi, C. Floriani, N. Re, A. Chiesi-Villa and C. Rizzoli, *J. Am. Chem. Soc.*, 1999, **121**, 2784; (*b*) L. Giannini, G. Guillemot, E. Solari, C. Floriani, N. Re, A. Chiesi-Villa and C. Rizzoli, *J. Am. Chem. Soc.*, 1999, **121**, 2797; (*c*) L. Giannini, S. Dovesi, E. Solari, C. Floriani, A. Chiesi-Villa and C. Rizzoli, *Angew. Chem., Int. Ed.*, 1999, **38**, 807; (*d*) L. Giannini, E. Solari, C. Floriani, N. Re, A. Chiesi-Villa and C. Rizzoli, *Inorg. Chem.*, 1999, **38**, 1438; (*e*) A. Caselli, E. Solari, E. Scopelliti and C. Floriani, *J. Am. Chem. Soc.*, 1999, **121**, 8296; (*f*) B. Castellano, E. Solari, C. Floriani, N. Re, A. Chiesi-Villa and C. Rizzoli, *Chem. Eur. J.*, 1999, **5**, 722.
3 (*a*) B. Castellano, E. Solari, C. Floriani, N. Re, A. Chiesi-Villa and C. Rizzoli, *Organometallics*, 1998, **17**, 2328; (*b*) A. Zanotti-Gerosa, E. Solari, L. Giannini, C. Floriani, N. Re, A. Chiesi-Villa and C. Rizzoli, *Inorg. Chim. Acta*, 1998, **270**, 298; (*c*) M. Giusti, E. Solari, L. Giannini, C. Floriani, A. Chiesi-Villa and C. Rizzoli, *Organometallics*, 1997, **16**, 5610; (*d*) A. Caselli, L. Giannini, E. Solari, C. Floriani, N. Re, A. Chiesi-Villa and C. Rizzoli, *Organometallics*, 1997, **16**, 5457; (*e*) L. Giannini, A. Caselli, E. Solari, C. Floriani, A. Chiesi-Villa, C. Rizzoli, N. Re and A. Sgamellotti, *J. Am. Chem. Soc.*, 1997, **119**, 9198; (*f*) L. Giannini, A. Caselli, E. Solari, C. Floriani, A. Chiesi-Villa, C. Rizzoli, N. Re and A. Sgamellotti, *J. Am. Chem. Soc.*, 1997, **119**, 9709; (*g*) B. Castellano, E. Solari, C. Floriani, R. Scopelliti and N. Re, *Inorg. Chem.*, 1999, **38**, 3406.
4 J. M. Thomas and W. J. Thomas, *Principles and Practice of Heterogeneous Catalysis*, VCH, Weinheim, 1997; H. H. Kung, *Transition Metal Oxides: Surface Chemistry and Catalysis*, Elsevier, Amsterdam, 1989; *Catalyst Design, Progress and Perspectives*, ed. L. Hegedus, Wiley, New York, 1987; G. C. Bond, *Heterogeneous Catalysis, Principles and Applications*, 2nd edn., Oxford University Press, New York, 1987.

5 A. Clark, *Catal. Rev.*, 1969, **3**, 145; F. J. Karol, G. L. Karapinka, C. Wu, A. W. Dow, R. N. Johnson and W. L. Carrick, *J. Polym. Sci., Part A-1*, 1972, **10**, 2621; F. J. Karol, G. L. Brown and J. M. Davison, *J. Polym. Sci., Polym. Chem. Ed.*, 1973, **11**, 413.
6 (*a*) B. J. Thomas and K. H. Theopold, *J. Am. Chem. Soc.*, 1988, **110**, 5902; (*b*) B. J. Thomas, S.-K. Noh, G. K. Schulte, S. C. Sendlinger and K. H. Theopold, *J. Am. Chem. Soc.*, 1991, **113**, 8983; (*c*) K. H. Theopold, R. A. Heintz, S.-K. Noh and B. J. Thomas, in *Homogeneous Transition Metal Catalyzed Reactions*, eds. W. R. Moser and D. W. Slocum, American Chemical Society, Washington, DC, 1992, p. 591.
7 V. C. Gibson, C. Redshaw, W. Clegg and M. R. J. Elsegood, *Chem. Commun.*, 1997, 1605.
8 E. A. Boudreaux and L. N. Mulay, *Theory and Applications of Molecular Paramagnetism*, Wiley, New York, 1976, pp. 491–495.
9 A. Arduini and A. Casnati, in *Macrocycle Synthesis*, ed. O. Parker, Oxford University Press, New York, 1996, ch. 7.
10 Z. Otwinowski and W. Minor, *Methods Enzymol.*, 1997, **276**, 307.
11 KM4RED DATA REDUCTION, version 1.5.8, KUMA diffraction instruments GmbH, PSE-EPFL module 3.4, Lausanne, 1999.
12 *International Tables for X-Ray Crystallography*, Kynoch Press, Birmingham, 1974, vol. IV, (*a*) p. 99; (*b*) p. 149.
13 R. F. Stewart, E. R. Davidson and W. T. Simpson, *J. Chem. Phys.*, 1965, **42**, 3175.
14 G. M. Sheldrick, SHELX 76, Program for crystal structure determination, University of Cambridge, Cambridge, 1976.
15 G. M. Sheldrick, SHELXL 93, Program for crystal structure refinement, University of Göttingen, Göttingen, 1993.
16 SCHAKAL 97, a computer program for the graphic representation of molecular and crystallographic models, E. Keller, *J. Appl. Crystallogr.*, 1989, **22**, 12.
17 J. Hvoslef, H. Hope, B. D. Murray and P. P. Power, *J. Chem. Soc., Chem. Commun.*, 1983, 1438; B. D. Murray, H. Hope and P. P. Power, *J. Am. Chem. Soc.*, 1985, **107**, 169; D. C. Bradley, R. C. Mehrotra and D. P. Gaur, *Metal Alkoxides*, Academic Press, London, 1978; R. C. Mehrotra, *Adv. Inorg. Chem. Radiochem.*, 1983, **26**, 269; M. H. Chisholm, F. A. Cotton, M. W. Extine and D. C. Redeout, *Inorg. Chem.*, 1979, **18**, 120.
18 C. D. Gutsche, *Calixarenes Revisited*, The Royal Society of Chemistry, Cambridge, 1998, ch. 6.
19 G. Bhandari, Y. Kim, J. M. McFarland, A. L. Rheingold and K. H. Theopold, *Organometallics*, 1995, **14**, 738; P. A. White, J. Calabrese and K. H. Theopold, *Organometallics*, 1996, **15**, 5473; M. J. Winter and S. Woodward, in *Comprehensive Organometallic Chemistry II*, eds. G. Wilkinson, F. G. A. Stone and E. W. Abel, Elsevier, Oxford, 1995, vol. 5, ch. 5.
20 E. S. Gould, *Coord. Chem. Rev.*, 1994, **135/136**, 651; D. A. House, *Adv. Inorg. Chem.*, 1997, **44**, 341.
21 C. J. O'Connor, *Prog. Inorg. Chem.*, 1982, **29**, 203; O. Kahn, *Molecular Magnetism*, VCH, Weinheim, 1993.
22 P. Knopp and K. Wieghardt, *Inorg. Chem.*, 1991, **30**, 4061 and references therein.
23 R. Hotzelmann and K. Wieghardt, *Inorg. Chem.*, 1993, **32**, 114.
24 R. Hoffmann and W. N. Lipscomb, *J. Chem. Phys.*, 1962, **36**, 2179; R. Hoffmann, *J. Chem. Phys.*, 1963, **39**, 1397.

Paper a908499a